Low-*Z* Element Analysis by Soft X-ray Line Emission of a Laser-produced Plasma

Hedser van Brug, Fred Bijkerk and Marnix J. van der Wiel
Association Euratom-FOM, FOM-Institute for Plasma Physics "Rijnhuizen," Edisonbaan 14, 3439 MN Nieuwegein, The Netherlands

Bob van Wingerden
Koninklijke/Shell Laboratory Amsterdam, Badhuisweg 3, 1031 CM Amsterdam, The Netherlands

A method for the rapid detection of low-*Z* elements in solid samples is presented. The detection is performed by measuring the characteristic soft X-ray line emissions of these elements in a plasma, produced by laser irradiation of the samples. A description is given of the determination of the Na and B contents of various samples which also contain C, H and O atoms. The signals are linear with respect to concentration up to 1 at.-%. In the experimental arrangement used, with its limited resolution, the detection limit for Na and B has been determined to be 0.04 at.-%. Therefore, there is the potential for an improvement in the detection limit by a factor of 40. A major restriction on the use of this method is the interference of emission lines, which is most likely to occur when high-*Z* elements are present in the samples.

Keywords: *X-ray emission; plasma; laser; low-Z elements*

For the multi-element analysis of samples containing low-*Z* elements only a limited number of techniques exist, each with its own characteristics. Examples of detection techniques commonly used for low-*Z* elements are inductively coupled plasma atomic emission spectrometry (ICP-AES)[1,2] and X-ray fluorescence (XRF) spectrometry.[3]

The ICP-AES technique is capable of determining elements down to the parts per billion (p.p.b.) level, but requires liquid samples. Other types of samples generally need to be converted into the liquid form (*e.g.*, by digestion), although methods for the direct introduction of solids have been reported (*e.g.*, thermal vaporisation[4] and laser ablation[1]). XRF can be applied to liquid and solid samples, but is restricted to elements with $Z > 10$, and the detection limits are in general at the parts per million (p.p.m.) level.

We present here a method for the detection of low-*Z* elements in solid samples, which was developed from studies of the production of laser-generated plasmas as a source of soft X-rays.[5] It has been found that, at laser irradiances of approximately 10^{12} W cm^{-2}, solid samples form plasmas which produce a clear and simple line emission spectrum for all elements from B to Si in the soft X-ray range (90–400 eV).

The determination of concentrations from line intensities has so far been applied to solid samples for elements up to $Z = 14$. For calibration purposes an internal standard was used. Elements with $Z > 14$ also produce line radiation, but either this lies outside the energy window, or the lines are too closely packed to be resolved at the resolution involved. Measurements on samples containing Ba showed that the low-*Z* elements (N and O) could not be detected in this high-*Z* containing matrix.

It is shown that the method is well suited for qualitative analysis of low-*Z* elements in a low-*Z* matrix. Limitations on the use for quantitative determinations are described.

Major restrictions on the use of this method are the interference of lines, the instability of the plasma parameters with changing sample conditions and the impossibility of measuring low-*Z* elements in a matrix of heavy elements. For our apparatus the upper limit for the matrix elements was $Z = 14$ owing to the poor resolution.

Experimental

The apparatus used is a frequency doubled Nd : YAG - glass laser system (15-ns pulses of 8 J of 532-nm light), a polychromator[6] and a multi-channel X-ray detector.[7] The laser pulse is focused on the sample surface to a spot of 65 μm diameter by a lens of 13 cm focal length. This yields a power density of approximately 10^{13} W cm^{-2} at the focus, which is high enough to produce a plasma. This plasma yields photons in the energy range 50–1000 eV, the soft X-ray region. An image of the plasma is created outside the source chamber by means of a collecting toroidal mirror. The X-ray beam is dispersed by a grating and the emission spectrum from 90 to 400 eV is recorded on a gold photoelectrode. Registration of the photoelectron yield across the full electrode on a position-sensitive detector provides the possibility of single-shot spectral measurements, with a 15-ns measuring time. The electron yield is recorded by a multi-channel plate - phosphor-screen assembly and an optical multi-channel detector. The positional information is held by a 0.12-T magnetic field.

The energy resolution of the apparatus is approximately 4 eV. The energy range of 250–800 eV can also be covered by changing the position of the gold photoelectrode. In Fig. 1 a schematic diagram of the apparatus is given. For more details see references 5–7. An essential feature of the apparatus is the possibility of making spatially resolved measurements, owing to the small probe area.

The following samples were investigated: $x\%$ *m/m* boric acid (H_3BO_3) in $(100 - x)\%$ *m/m* cellulose ($C_6H_{10}O_5$) and $x\%$ *m/m* sodium nitrate ($NaNO_3$) in $(100 - x)\%$ *m/m* cellulose, where x = 0,1,3,7,10,30,70 or 100. After mixing the two powders in the correct ratio, the mixture was compressed into a pellet. The pressure used was 20 tons on a circular surface with a diameter of 4 cm. These pellets were used as targets for the laser beam to produce the X-ray emitting plasmas. In the X-ray production mechanism, the relative number of atoms of an element is considered to be, to a first approximation, a measure of the relative intensity of the emitted line. Therefore, we calculated the atomic percentages (at.-%) of the elements in the mixtures. The results are given in Table 1.

The reproducibility of the spectra, defined here as the difference in intensity in one spectral channel between a single-shot measurement and the mean value, measured over a large number of shots (more than 10), is better than 10%. The peak-to-peak and the peak-to-background reproducibility of the spectra were determined to be approximately 3%. This value is of more importance in this method than the shot-to-shot reproducibility, as we use the ratio between the heights of two peaks and not the absolute peak height. The 3% variations are probably due to the fluctuation in the laser output and the inhomogeneity of the sample. Measurements on glassy and metallic samples showed a peak-to-peak and peak-to-background reproducibility of better than 1%. This indicates that the poor reproducibility obtained with the compressed powders is caused by their inhomogeneity.

We measured the X-ray emission spectra as a function of the percentage of boric acid and sodium nitrate in cellulose. We recorded the X-ray emission spectra of 30% *m/m* sodium nitrate in 70% *m/m* cellulose as a function of the power density in the laser focus at constant focus size. In all instances, averaged measurements for five spectra were taken in order to improve the statistics and to cancel partially the effects of the inhomogeneities in the samples. Measurements on fluorine-containing samples were also performed but will not be considered here. However, we can state that this method is capable of detecting fluorine.

Results

In Figs. 2 and 3 the spectra of various amounts of boric acid and sodium nitrate in cellulose are given. In Table 2 the observed peaks in Figs. 2 and 3 are assigned as emission lines from C, B, Na and O. For the assignment we used the tables of Kelly.[8]

In the following discussion, intensity represents the height of an emission line after background subtraction. The backgrounds for the B, C and Na peaks were determined by recording a "zero" spectrum, *i.e.*, a spectrum without the element under investigation. For oxygen peaks the background was determined visually. The error in the peak-height determination due to the background subtraction was *ca.* 5–10% for oxygen peaks, whereas for the other peaks errors as small as 2% could be obtained.

The detection limit, defined as the 3σ value, was determined to be 0.04 at.-% for both B and Na in this type of matrix. The σ value is the r.m.s. value of the noise in the spectrum in the energy range of the peak when the element is not present. To determine the detection limit, we used the strongest lines of B and Na, *i.e.*, in the notation of Table 2, B^3 and Na^6. This detection limit is valid for the resolution of 4 eV. A better detection limit can be obtained if the resolution is improved, and the best possible detection limit is obtained if the resolution is better than the line widths. The line widths of the transitions under investigation are of the order of 0.1 eV. This indicates that in theory a detection limit of *ca.* 0.001 at.-% would be obtainable, which is an improvement by a factor of 40. One way to obtain this better resolution, in our apparatus with the given dimensions, could be to use a better focusing lens in order to obtain a smaller plasma size. However, good lenses, capable of handling high-power laser beams are

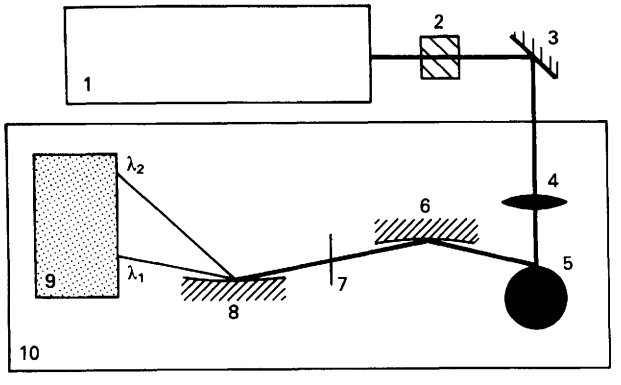

Fig. 1. Schematic diagram of the apparatus: 1, Nd : YAG - glass laser system; 2, second harmonic generator; 3, beam splitter; 4, lens with a focal length of 13 cm; 5, laser target, *i.e.*, position of sample; 6, toroidal mirror; 7, 50-μm slit for plasma size determination; 8, concave grating; 9, multi-channel detector; and 10, vacuum system, *ca.* 10^{-6} Pa

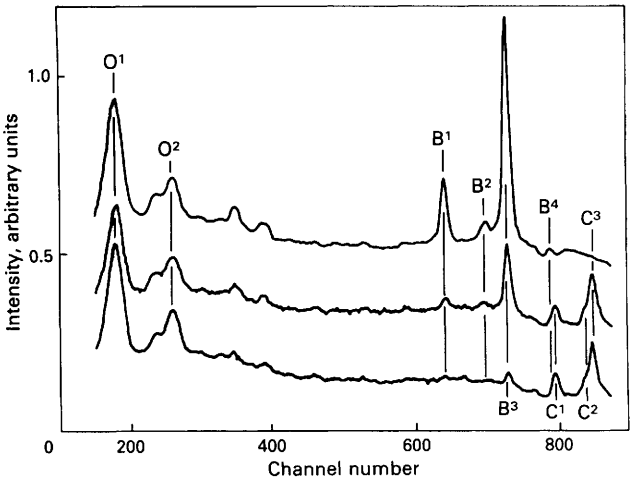

Fig. 2. X-ray emission spectra for mixtures of 100, 10 and 1% *m/m* H_3BO_3 in $C_6H_{10}O_5$. The 100 and 10% *m/m* spectra are shifted upwards for clarity. Spectra recorded at a power density in the laser focus of *ca.* 10^{13} W cm^{-2}

Table 1. Atomic percentages in the compound as calculated from the percentages by mass of the two elements

Percentages of H_3BO_3 (x% *m/m*) *in* $C_6H_{10}O_5$ (100 − x% *m/m*)—

	x, % *m/m*							
Element	0.0	1.0	3.0	7.0	10.0	30.0	70.0	100.0
B	0.00	0.12	0.38	0.88	1.26	3.89	9.58	14.29
O	23.81	23.98	24.31	24.99	25.50	29.00	36.59	42.86
C	28.57	28.32	27.82	26.81	26.04	20.79	9.40	0.00

Percentages of $NaNO_3$ (x% *m/m*) *in* $C_6H_{10}O_5$ (100 − x% *m/m*)—

	x, % *m/m*							
Element	0.0	1.0	3.0	7.0	10.0	30.0	70.0	100.0
Na/N	0.00	0.09	0.28	0.66	0.96	3.26	10.29	20.00
O	23.81	23.97	24.31	25.00	25.55	29.70	42.42	60.00
C	28.57	28.44	28.18	27.63	27.20	23.92	13.88	0.00

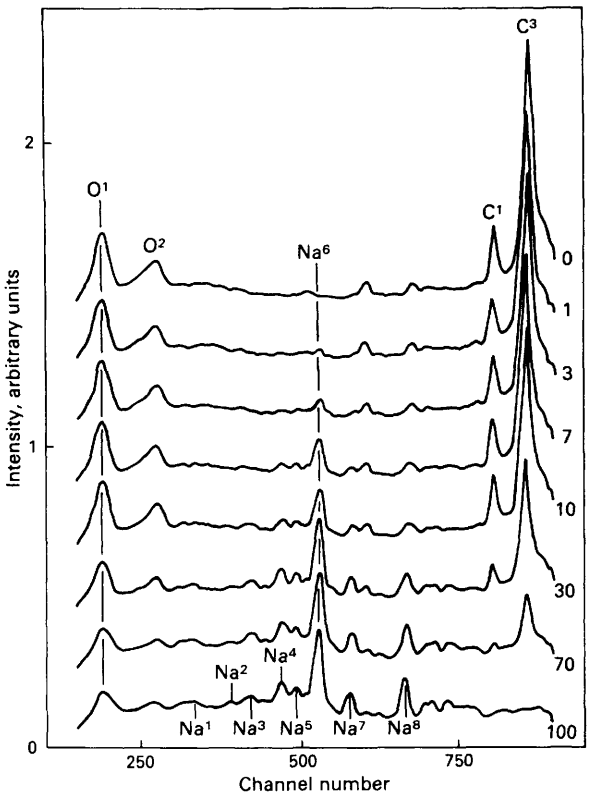

Fig. 3. X-ray emission spectra for various concentrations of $NaNO_3$ in $C_6H_{10}O_5$ recorded at a power density of *ca.* 10^{13} W cm^{-2}. Concentrations of $NaNO_3$ in $C_6H_{10}O_5$ from 0 to 100% *m/m*. All curves except that for 100% *m/m* are shifted upwards for clarity

Table 2. Assignment of the main emission lines. For each line the transition, the energy value and the ionisation state are given[8]

Emission line	Transition	Energy/ eV	Ionisation state
B^1	1s^2 - 1s2p	205.6	B IV
B^2	1s^2 - 1s3p	235.4	B IV
B^3	1s - 2p	255.2	B V
B^4	1s - 3p	302.4	B V
C^1	1s^2 - 1s2p	307.9	C V
C^2	1s^2 - 1s3p	354.5	C V
C^3	1s - 2p	367.5	C VI
O^1	1s^{2}2p - 1s^{2}4d	95.5	O VI
O^2	1s^{2}2p - 1s^{2}5s	105.6	O VI
O^3	1s^{2}2p - 1s^{2}5d	106.5	O VI
O^4	1s^{2}2s - 1s^{2}4p	107.1	O VI
Na^1	2s2p^2 - 2s2p3d	112.0	Na VII
Na^2	2s2p^2 - 2s2p3d	124.6	Na VII
Na^3	2s^{2}2p - 2s^{2}3d	131.4	Na VII
Na^4	2p^2 - 2p3d	143.4	Na VIII
Na^5	2s2p - 2s3d	148.9	Na VIII
Na^6	1s^{2}2p - 1s^{2}3d	159.2	Na IX
Na^7	1s^{2}2s - 1s^{2}3p	175.6	Na IX
Na^8	1s^{2}2p - 1s^{2}4d	212.9	Na IX

difficult to acquire. A different way to improve the resolution might be to use a grating with a higher line density.

The results of the emission measurements as a function of the power density at the laser focus are presented in Fig. 4. These spectra were all recorded on the same sample, namely 30% *m/m* sodium nitrate in 70% *m/m* cellulose. For every shot a fresh area of sample surface was exposed to the laser beam, keeping the point of emission fixed with respect to the polychromator. The power density was changed by decreasing the voltage on the final amplifier of the laser. The spectra measured at different power densities were expressed

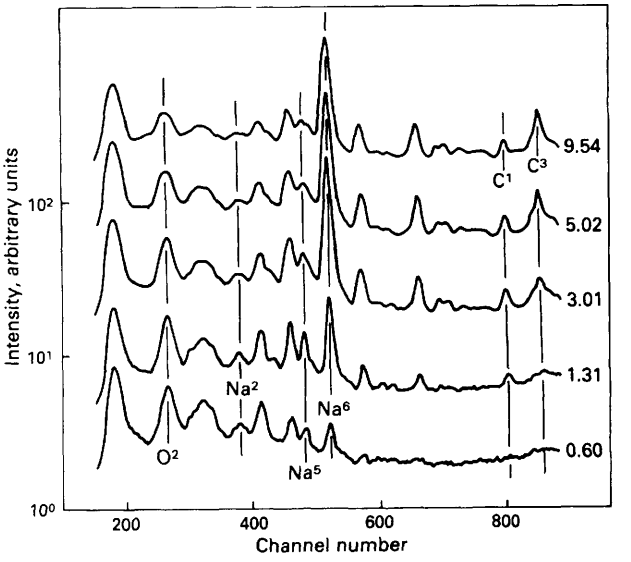

Fig. 4. X-ray emission spectra of 30% *m/m* $NaNO_3$ in 70% *m/m* $C_6H_{10}O_5$ for different power densities in the laser focus. Power densities used ($\times 10^{12}$ W cm^{-2}) are given on the right of each curve. The logarithms of the emission spectra were taken before plotting the curves, in order to cancel the over-all scaling effects due to the change in power density

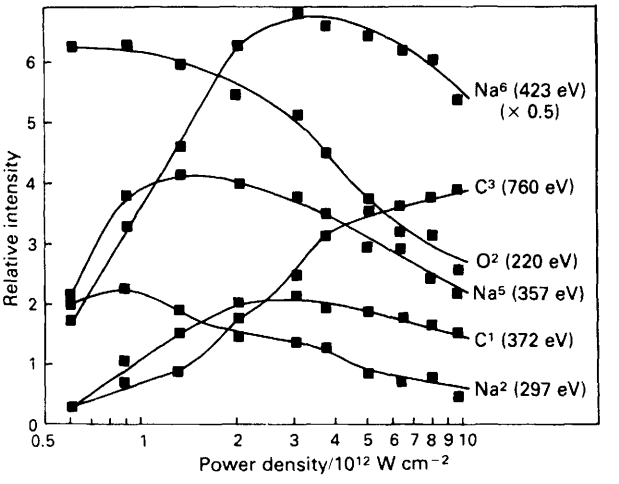

Fig. 5. Relative intensity of emission peaks above background level measured for the curves in Fig. 4, as a function of the power density in the laser focus

logarithmically. This method of representation ensured that the over-all variation in the spectrum as a function of power density showed up as an offset with respect to the zero level. The line intensities could then be measured as a function of the power density for all lines. The results are given in Fig. 5, from which it can be seen that some lines decrease with increasing power density. On the right of the curves the total energy required to produce the transition involved is indicated. This is the transition energy plus the energy needed to make the last, and largest, ionisation step to reach the ionisation level from which the transition occurs. It can be seen that lines that require a higher total energy have their maximum at a higher power density, and therefore at a higher plasma temperature. A further discussion of Fig. 5 is given later.

From the power dependence measurements we can conclude that when five spectra are averaged, the laser needed has a minimum output power of 6×10^{11} W cm^{-2} ($\approx$0.4 J of output energy of 532-nm light), with the given pulse duration of 15 ns. At this power density the photon flux is *ca.* 10^6 photons per pulse. At a lower output power the photon flux of the plasma becomes too low.

Discussion

For practical purposes, in a quantitative analysis method it is preferable to work with an internal reference, such that

$$X\,(\text{at.-\%}) = \left(\frac{I_Y}{I_X}\right)[Y\,(\text{at.-\%})]\,Q\,(X\,\text{at.-\%}) \quad . . \quad (1)$$

where X represents the element to be detected, Y the internal standard needed for the scaling of the spectra and I_X and I_Y the intensities, *i.e.*, the height of the particular line of element X or Y, above the background level, used in the analysis. The calibration factor Q should be a constant for all X at.-% values in an ideal case.

Using equation (1) we calculated Q from the spectra when X = Na or B and Y = O. When X = Na, equation (1) can be written as

$$Q(\text{Na at.-\%}) = \left\{\frac{[\text{Na (at.-\%)}]}{I_{\text{Na IX}}}\right\}\left\{\frac{I_{\text{O VI}}}{[\text{O (at.-\%)}]}\right\} \quad . . \quad (2)$$

The Roman numbers after the element names indicate the ionisation state from which the line emission originates (*e.g.*, Na IX represents Na^{8+}). The results for Q are shown in Fig. 6, from which it is clear that Q is not a constant. In Fig. 6 the error bars have been left out for clarity. The error in the determination of Q is approximately 10%, increasing to 15% for concentrations below 1 at.-%, caused by the uncertainty in the determination of the background contribution. The background is caused by recombination radiation and bremsstrahlung in the plasma, the continuum part of the spectrum, plus the scattering from optical components and slits in the polychromator.

The fact that Q is not constant can have two possible causes. The first is that the ratio between the number of Na IX ions and the total number of Na atoms plus ions is not proportional to the ratio between the number of O VI ions and the total number of O atoms plus ions as the sodium nitrate concentration changes. This is a result of changes in the plasma temperature, T_e, and the electron density, n_e. The second cause is the self-absorption of the plasma; the observed line intensity is not a measure of the abundance of an atom as the emitted X-rays can be absorbed by other elements. These two causes will be elaborated upon in the ensuing discussion, as it is to be expected that both are operative.

In equations (1) and (2) only the dependence of Q on Na at.-% and O at.-% has been expressed explicitly. However, Q is also dependent on the amounts of H, C and N in the sample; this dependence is discussed below.

As Q is not constant, then, owing to the first of the two reasons mentioned above, the ratio of Na IX to O VI must be different from the ratio of the total number of neutral atoms plus ions in all ionisation states of Na to the corresponding total number for O as the amount of Na in the sample changes. The ratio of Na IX ions to the total Na can be determined if the electron temperature and the electron density in the plasma are known. The technique for determining the ratio is explained qualitatively below.

We calculated the abundances $N(T_e, n_e, Z)$ of O and Na in various ionisation states as a function of the electron temperature, assuming the collisional - radiative (CR) model in reference 9 to be valid, and using the stationary-state description in that reference. The abundance is given by

$$N(T_e, n_e, Z) = \frac{n(T_e, n_e, \xi)}{\Sigma n(T_e, n_e, \xi)} \quad . . \quad . . \quad (3)$$

where n is the number of atoms in a given ionisation state ξ, and the summation is performed from $\xi = 0$ to Z, *i.e.*, over all possible ionisation levels. The result of the summation has been normalised and the results of the calculations are shown in Fig. 7. The electron density, n_e, was taken as constant at

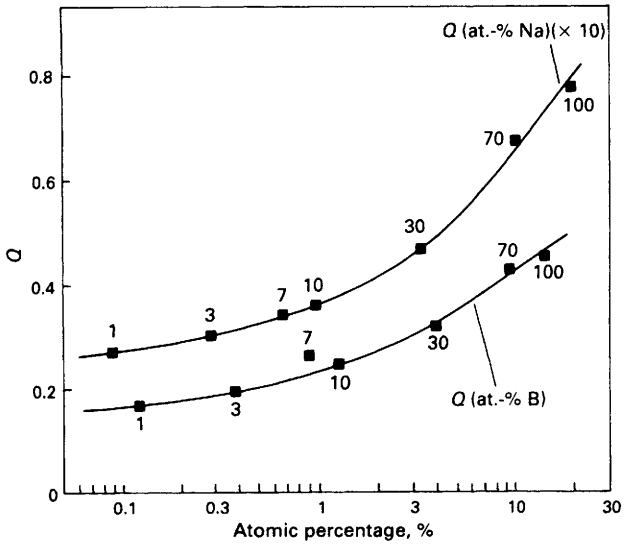

Fig. 6. Calibration factor Q *versus* atomic percentage for both Na and B. These curves were obtained from measurements at *ca.* 10^{13} W cm^{-2}. The error bars are omitted for clarity. The error in the determination of Q is *ca.* 10%

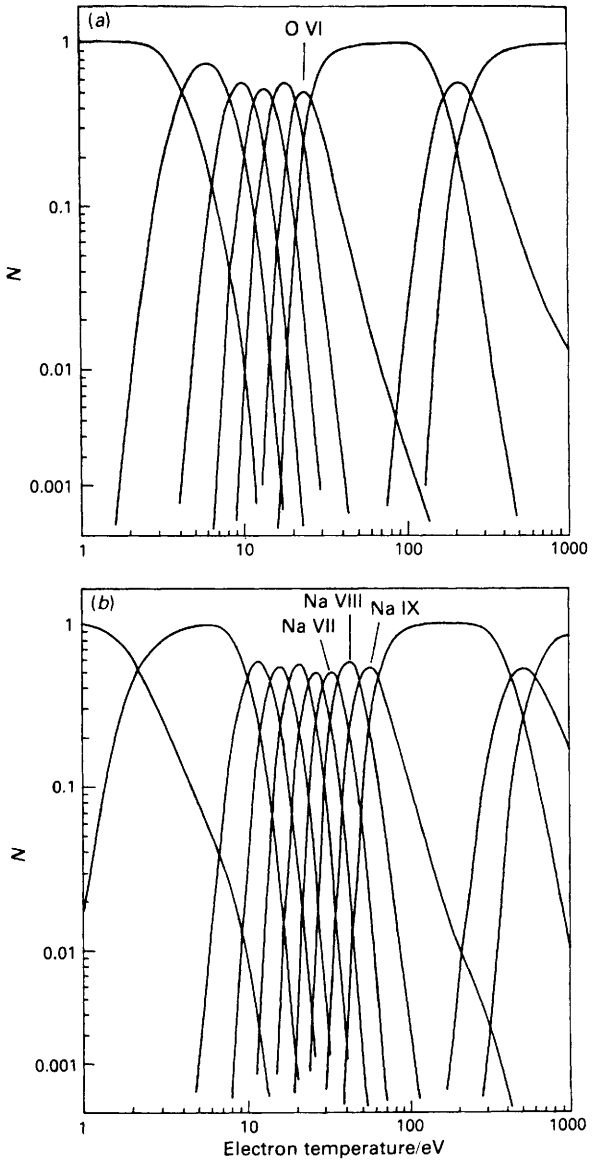

Fig. 7. Abundance $N(T_e, n_e, \xi)$ *versus* T_e for (*a*) oxygen and (*b*) sodium

10^{21} cm^{-3}, which, according to Colombant and Tonon,[9] is a good approximation for a plasma created by an Nd:YAG - glass laser. Combining the results of the power dependence measurements and these distribution curves, we conclude that, under the assumptions needed for the CR model, the plasma temperature at a laser energy of 3×10^{12} W cm^{-2} is approximately 60 eV. This was done by measuring the power density at which the Na^6 line, originating from Na IX, reaches its maximum.

Fig. 5 shows the abundance of ionisation states, by showing the peak heights for different ionisation levels of different elements. It can be seen that, on increasing the power density, the peak heights of ions with a higher charge gain intensity at the expense of the peak heights of ions with a lower charge.

The measurements as a function of the percentage of sodium nitrate in the sample were performed at a power density of about 10^{13} W cm^{-2}. From Fig. 6 it can be seen that the relative intensity of the Na^6 line increases with decreasing amount of sodium nitrate in the sample. This can be explained by a decrease in electron temperature, T_e, when the amount of sodium nitrate decreases, as the power density dependence measurements show an increase in the intensity of the Na^6 line when the power density, and thus T_e, was lowered. A reason for the decrease in the electron temperature can be found from a scaling law for T_e[9]:

$$T_e \approx 5.2 \times 10^{-6} Z^{1/5} \lambda^{6/5} \Phi^{3/5} \quad \ldots \quad (4)$$

where Z is the mean atomic number of the elements present in the sample, λ is the wavelength of the laser light in μm and Φ is the laser output flux in W cm^{-2}. Calculation of the mean atomic number gives 4.1 for cellulose, 8.4 for sodium nitrate and 4.6 for boric acid. This indicates a decrease in the mean Z value if the amount of cellulose in the sample is increased, yielding a lower value for T_e. In this discussion the change in the intensity of oxygen has been neglected. When oxygen is included the relative rise in the Na^6 intensity must be larger than that in the O^1 intensity with a decrease in the amount of sodium nitrate in the mixture, which, in Fig. 7, can be seen to be the case for the T_e values of interest.

The second possible cause of the dependence of Q on X is self-absorption in the plasma. A given line of an element A can be absorbed by an element B and produce an increase in the height of a B line at lower energy. The result of this process is a transfer of intensity from A to B. This would yield an increase in intensity of the Na^6 line at higher densities of carbon, as observed in Fig. 6. This explanation can also be used for the B^3 and C^3 lines. The effect of the density of carbon on the line heights of oxygen is not as great because the energy difference between the oxygen and carbon transitions is larger than that between those of sodium and carbon.

Soft X-ray line emission of a laser-produced plasma can be used for quantitative analysis with certain restrictions. From Fig. 6 it can be seen that Q is constant to within 10% for concentrations of the element to be detected of up to 1 at.-%. For these low concentrations of X the plasma conditions will hardly change for different samples. The detection limit was determined, for the resolution obtained, to be 0.04 at.-%. This gives a measurement range from 0.04 to 1 at.-%. For measurements in this range the amount of element Y must be known, then the amount of X can be calculated using equation (1). For measurements at higher percentages this method can only be used when series of reference samples can be used for calibrations. Once the calibration of Q has been made at a given output power of the laser, the output must be kept constant in order to obtain the same plasma conditions for the measurements as during the calibration procedure. Our laser output has an output power variation of 5% after frequency doubling, which was found to be sufficiently stable for this method.

Conclusions

Low-Z element analysis ($Z \leqslant 14$) by characteristic line emission of a laser-produced plasma can be applied for the detection of these elements in a sample. We established a detection limit of 0.04 at.-% for both boron and sodium in a cellulose matrix. It is expected that the detection limit is element dependent. For resolutions smaller than the line width the detection limit can potentially be improved by a factor of 40.

The results have shown that the method is semi-quantitative for concentrations below 1 at.-%. For higher concentrations the method will have to rely on calibration by means of a series of reference samples.

Restrictions on the use of this method are the interferences between emission lines, most strongly present for high-Z elements ($Z > 14$), and the changes in plasma parameters resulting from changes in the target conditions. The low-Z elements N and O could not be detected in a matrix containing barium.

For this method a small laser system can be used with an output energy of approximately 0.4 J of 532-nm light in 15 ns.

The authors thank T. Hoekstra of the Koninklijke/Shell Laboratory in Amsterdam for the sample preparation, and R. Koper and R. Kemper for technical assistance. This work is part of the research programme of the association Euratom-FOM (Foundation for Research on Matter) and was made possible by financial support from the Nederlandse Organisatie voor Zuiver-Wetenschappelijk Onderzoek (Netherlands Organization for the Advancement of Pure Research).

References

1. Carr, J. W., and Horlick, G., *Spectrochim. Acta, Part B*, 1982, **37**, 1.
2. Ishizuka, T., and Uwamino, Y., *Spectrochim. Acta, Part B*, 1983, **38**, 519.
3. Raith, B., Roth, M., Göllner, K., Gonsior, B., Ostermann, H., and Uhlhorn, C. D., *Nucl. Instrum. Methods*, 1977, **142**, 39.
4. Matusiewicz, H., *J. Anal. At. Spectrom.*, 1986, **1**, 171.
5. Gerritsen, H. C., van Brug, H., Bijkerk, F., and van der Wiel, M. J., *J. Appl. Phys.*, 1986, **59**, 2337.
6. Gerritsen, H. C., van Brug, H., Beerlage, M., and van der Wiel, M. J., *Nucl. Instrum. Methods*, 1985, **238A**, 546.
7. Gerritsen, H. C., van Brug, H., Bijkerk, F., and van der Wiel, M. J., *J. Phys. E.*, 1986, **19**, 1040.
8. Kelly, R. L., "Atomic and Ionic Emission Line Below 2000 Å," ORNL Report 5922, Controlled Fusion Atomic Data Center, Physics Division, Oak Ridge National Laboratory, Oak Ridge, TN, 1982.
9. Colombant, D., and Tonon, G. F., *J. Appl. Phys.*, 1973, **44**, 3524.

Paper J6/126
Received December 29th, 1986
Accepted March 2nd, 1987